# Elasticity Estimation for Sample by AFM Utilizing Previous Line Sample Surface Topography

Sakiya Watanabe and Hiroshi Fujimoto
Department of Electrical Engineering, The University of Tokyo
5-1-5, Kashiwanoha, Kashiwa, Chiba, 277-8561, Japan
Phone: +81–4–7136–3881, Fax: +81–4–7136–3881
Email: watanabe@hflab.k.u-tokyo.ac.jp, fujimoto@k.u-tokyo.ac.jp

*Abstract*— **Atomic Force Microscope (AFM) is a device which can be applied to measure the surface topography of sample in nano–scale. Because cantilever holds its physical contact with the sample, it is also possible to measure the elasticity of samples in principle. However, in comparison with the improvement of scanning performance, the technologies for viscosity and elasticity measurement are still underdeveloped. In this paper, we propose a method which can measure both the surface topography and the elasticity of samples. Recursive least–square approach is applied to estimate the elasticity of samples using the information of the previous surface topography.**

## I. INTRODUCTION

The rapid development of the atomic and molecular electronics, including more and more powerful microprocessors, contributes to the development of many fields like informatics, biotechnologies, etc. Atomic Force Microscope (AFM), which can measure the surface topography of samples in nano–scale, is one of the milestone products of the development.

Thanks to the feature of holding a physical contact with samples, AFM can detect atomic force between atoms. Therefore, unlike Scanning Tunneling Microscope (STM) whose samples should be conductive materials, AFM does not have much restriction on sample materials. Furthermore, AFM contributes to nano–manipulation using bilateral control because of broad utility[1]. In accuracy measurement, it is known that conventional feedback control methods result in time–consuming of measurement. In order to improve scanning speed and accuracy, many method have been proposed from the view point of hardware and control theory[2][3][4][5]. The authors' research group has applied learning control method, as well as observer and Perfect Tracking Control (PTC) on AFM, and fast and precise scanning control is obtained[6][7].

In this paper, we deal with measuring the sample's elasticity using AFM. In many cases, material elasticity and viscosity are important information, especially when measuring soft materials like protein. In addition, it would be able to develop a new material if the characteristic of the sample is known. There are several studies on measuring the elasticity and viscosity of samples using AFM, for instance, analysis of the force–distance curve[8][9], or measuring of sample's elasticity by Recursive Least Square (RLS) method[10]. However, sample's elasticity and viscosity measurement technique has not been developed as the high speed scanning and high accuracy measurement techniques[11].

Literature reviews show that it is rare to find the works on measuring the surface topography and elasticity at the same time. Moreover, the dynamics of piezo actuator is not taken into account. In this paper, we propose a method which can measure sample's surface topography and elasticity in alternate shifts. In this method, we switch the reference signal of AFM in order to reduce the influence of unknown noise. In addition, we use RLS method in order to get higher reproducible and accuracy results.

## II. ATOMIC FORCE MICROSCOPE

In this section, we introduce our experiment device and AFM. There are basically two types of AFM, one is contact–mode AFM, the other is Dynamic–mode AFM. Contact–mode AFM can measure samples accurately, and its physical model is simpler than dynamic–mode AFM. In this paper, we only consider contact–mode AFM.

### A. *Contact–mode AFM*

In general there are two ways to measure the displacement of cantilever by surface topography. The former is a method to measure the interference of laser beams (optical interferometry). The later is a method to measure the reflection angle of laser beam (optical lever method). In this paper, we use the optical lever method. As shown in Fig. 1, in the optical lever method, the relative change of optical strength is measured by photo diodes. The bend of the cantilever tip by the sample surface topography can be detected by the photo diodes, then compensated by feedback controller moving piezo stage in Z–direction.

Fig. 2 shows the surface scan route of the cantilever. The scan route consists of forward scan (FWS) and backward scan (BWS). In FWS, AFM scans the sample from left to right. In BWS, it scans on the same route from right to left. The sample image is obtained by scanning in FWS and BWS repeatedly in Y–direction. In this paper, we consider only FWS, and the sample surface topography in the $i$ row is defined as $d_i$.

### B. *Physical model of contact–mode AFM*

In this paper, we assume that sample's viscosity can be neglected. Then, Fig. 3 shows the physical model of contact–mode AFM[12], where $m$, $b$, $k$, $d$, $k_a$, $z$, and $u$ denote mass of the cantilever, viscosity coefficient of the cantilever, spring

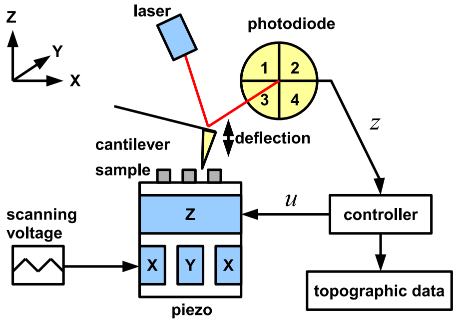


Fig. 1. Optical lever method (AFM).

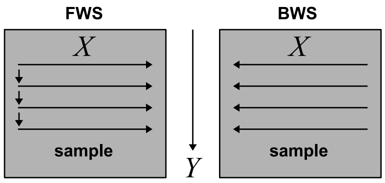


Fig. 2. Surface scan route of the cantilever.

constant of the cantilever, spring constant of the sample elasticity, displacement of the surface topography, and input for piezo actuator in Z–direction, respectively. Thus, the motion equation of the cantilever is represented by

$$z = \frac{k_a}{ms^2 + bs + (k + k_a)}(u + d). \quad (1)$$

Without loss of generality, we assume that the spring constant of the sample is far smaller than that of the cantilever, in other words, ($k_a \ll k$). Following this assumption, eq. (1) is rewritten as

$$z \simeq \frac{k_a}{ms^2 + bs + k}(u + d). \quad (2)$$

In the acutual AFM, there is a scale setting gain $g$ when displacement is detected by photo diodes. Transfer function of contact–mode AFM is rewritten as

$$\begin{aligned} P(s) &= \frac{z}{u} = g\frac{k_a}{ms^2 + bs + k} \\ &= \frac{k'_a}{s^2 + b's + k'}(u + d), \end{aligned} \quad (3)$$

where $k' = \frac{k}{m}$, $b' = \frac{b}{m}$, $k'_a = g\frac{k_a}{m}$.

### C. Experimental setup

Our experimental setup, JSPM–5200 manufactured by JEOL Ltd., is customized as shown in Fig. 4. The controllers of commercial AFM are generally in black box. Therefore, users cannot implement their own control algorithm. Our control algorithm is implemented and verified in a DSP–based–control–system.

Fig. 5 shows the typical block diagram of AFM. In Fig. 5, the controller used in the commercial product is an analog

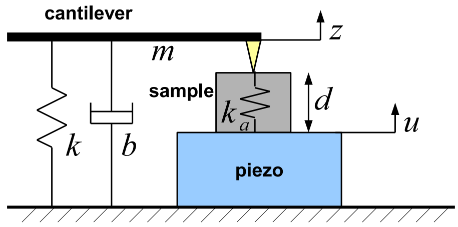


Fig. 3. Model of contact–mode AFM.

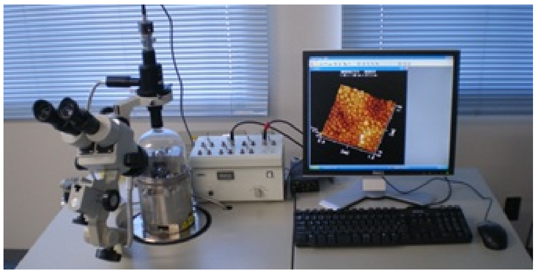

Fig. 4. Experimental device.

phase–lag compensator,

$$C(s) = \frac{\omega_c}{s + \omega_c}k_p. \quad (4)$$

The paramertor are tuned as $k_p = 100$, $\omega_c = 2\pi f_c$ ($f_c = 0.5$ Hz based on the manual of JSPM–5200.

We use the plastic sample as for measurement. Fig. 6 shows the frequency response, which is the response from input $u$ to the cantilever position $z$, and attained by using a servo analyzer. According to Fig. 6, we can attain the nominal plant as

$$P_n(s) = \frac{1.245 \times 10^8}{s^2 + 6.377 \times 10^3 s + 8.300 \times 10^7}. \quad (5)$$

However, eq. (5) is true for a point of the sample. Usually, spring constant of the sample differs from one locating to another. Therefore, accurate elasticity estimation at every points of samples is important.

## III. Elasticity Estimation Using Recursive Least Square

Spring constant of the sample, $k_a$, is not necessary to be constant in the same sample. It can be different at each point. We use RLS method in order to measure the sample's spring constant accurately. Generally, plant input $u + d$ is very small because AFM scans the sample at a reference of $r = 0$. This causes small S/N ratio, then the sample's spring constant can not be estimated accurately. In this section, we propose the estimation method switching the reference signal $r$ of AFM in order to increase the S/N ratio and improve the estimation accuracy.

### A. Recursive least square

RLS is a method to identify parameters of system[13]. In this subsection, we introduce the algorithm of RLS.

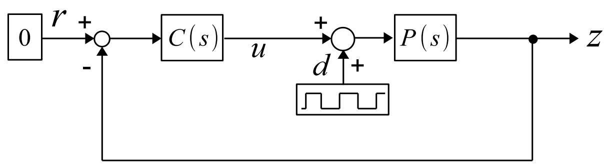


Fig. 5. Block diagram of AFM.

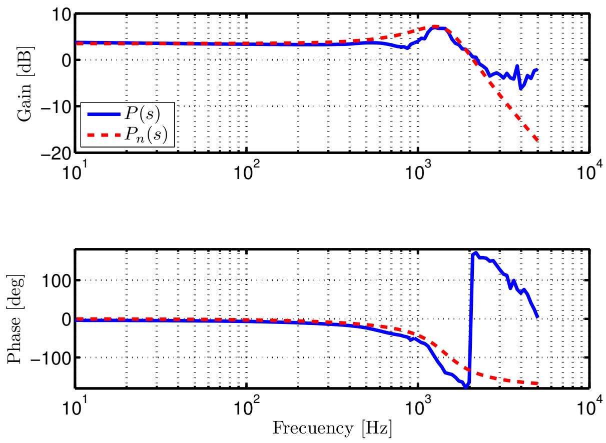


Fig. 6. Frequency response of the plastic sample.

Input–output relation is denoted by

$$\begin{aligned} y[k]+a_1y[k-1]+\cdots+ \quad a_{n_a} \quad & y[k-n_a] \\ =b_1u[k-1]+ \quad \cdots \quad & +b_{n_b}u[k-n_b]. \end{aligned} \tag{6}$$

Then, eq. (6) is rewritten as

$$y[k]=\boldsymbol{\theta}^{\mathrm{T}}[k]\boldsymbol{\varphi}[k], \tag{7}$$

where $\boldsymbol{\theta}[k]$ and $\boldsymbol{\varphi}[k]$ are the unkown parameter vector and the regression vector defined as

$$\boldsymbol{\theta}[k] = [a_1,...,a_{n_a},b_1,...,b_{n_b}]^{\mathrm{T}}, \tag{8}$$

$$\boldsymbol{\varphi}[k] = [-y[k-1],...,-y[k-n_a],u[k-1],...,u[k-n_b]]^{\mathrm{T}}. \tag{9}$$

Using RLS algorithm, the estimation of the unknown parameter vector $\boldsymbol{\theta}[k]$ is denoted by

$$\hat{\boldsymbol{\theta}}[k] = \hat{\boldsymbol{\theta}}[k-1]+\frac{\boldsymbol{P}[k-1]\boldsymbol{\varphi}[k]}{\lambda+\boldsymbol{\varphi}[k]^T\boldsymbol{P}[k-1]\boldsymbol{\varphi}[k]}\epsilon[k], \tag{10}$$

$$\epsilon[k] = y[k]-\boldsymbol{\varphi}^T[k]\hat{\boldsymbol{\theta}}[k-1], \tag{11}$$

$$\boldsymbol{P}[k] = \frac{1}{\lambda}\Big(\boldsymbol{P}[k-1],-\frac{\boldsymbol{P}[k-1]\boldsymbol{\varphi}[k]\boldsymbol{\varphi}^T[k]\boldsymbol{P}[k-1]}{\lambda+\boldsymbol{\varphi}^T[k]\boldsymbol{P}[k-1]\boldsymbol{\varphi}[k]}\Big), \tag{12}$$

where $\lambda$ is the forgetting factor $(0<\lambda\leq 1)$, $\hat{\boldsymbol{\theta}}[0]=0$, and $\boldsymbol{P}[0]=\gamma\boldsymbol{I}(0<\gamma)$.

### B. Proposed elasticity estimation method

In this subsection, sample elasticity estimation method is proposed using a previous line sample surface topography. In the contact–mode AFM, the bend of cantilever is compensated by feedback controller. Then, the $i$ th row surface topography is denoted by

$$\hat{d}_i=-u_i. \tag{13}$$

We assume that the sample is satiny and the $i$th row is closed to the $(i-1)$th line in FWS. That is

$$d_i=d_{i-1}+\Delta_{i-1}, \tag{14}$$

where $\Delta_{i-1}$ is the difference between the $i$th line and the $(i-1)$th line surface topography. Eq. (3) is rewritten as

$$\begin{aligned} Q(s)\Big(s^2+b's+k'\Big)z &= Q(s)\left[k'_a(u_i+d_i)\right] \\ &= Q(s)\left[k'_a(u_i-u_{i-1}-\Delta_{i-1})\right], \end{aligned} \tag{15}$$

where $Q(s)=\frac{\omega_f^2}{(s+\omega_f)^2}$ is the low–pass filter to make the left side of (15) proper ($\omega_f=100$ rad/s).

Eq. (15) is rewritten as

$$y = \theta^{\mathrm{T}}\varphi+e, \tag{16}$$

where,

$$\theta = k'_a, \tag{17}$$

$$\varphi = Q(s)(u_i-u_{i-1}), \tag{18}$$

$$y = Q(s)\Big(s^2+b's+k'\Big)z, \tag{19}$$

$$e = Q(s)k'_a\Delta_{i-1}. \tag{20}$$

From (1), the denominator coefficient of the transfer function is independent on spring constant of sample $k_a$, when spring constant of sample is far smaller than that of the cantilever. Therefore, the following equation can be obtained,

$$\frac{k}{m} = 8.300\times 10^7, \tag{21}$$

$$\frac{b}{m} = 6.377\times 10^3. \tag{22}$$

Thus, we can estimate sample's spring $\theta$ and surface topography $d$ using RLS method.

From (13), (14), $\varphi$ is expressed by

$$\begin{aligned} \varphi &= Q(s)(u_i-u_{i-1}) \\ &\simeq 0. \end{aligned} \tag{23}$$

In actual measurement, output is corrupted by noise. The S/N ratio is small when input signal is too small. Thus, such exact estimation results is obtained only when input signal is large. From Fig. 5, the S/N ratio is improved when a proper reference is given. However, this means that the cantilever pushes a sample strongly. The material which needs elastic measurement is soft, hence, elastic deformation arise between them. Furthermore, the soft material may be destroyed by the

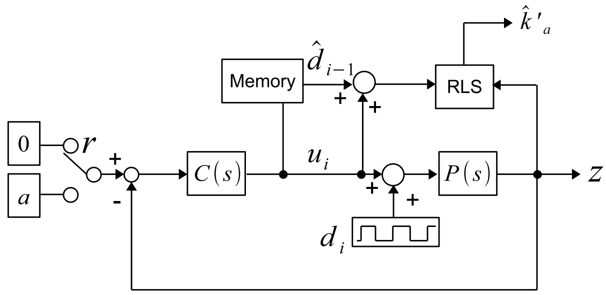


Fig. 7. Block diagram of the proposed method.

force from the cantilever. Therefore, it is undesirable to have a reference with large magnitude.

We propose that the reference $r$ is changed from 0 to $a$ for every sequence. Fig. 7 shows the block diagram of the proposed method. In this case, plant input $u_i$ is expressed by

$$u_i = \frac{C}{1+PC}r - \frac{CP}{1+PC}d_i, \tag{24}$$

$$r = \begin{cases} 0 & \text{if } i \text{ is odd,} \\ a > 0 & \text{if } i \text{ is even,} \end{cases} \tag{25}$$

where $a$ is the value not to cause too large elastic deformation.

In this method, S/N ratio can be improved, and the damage given to the sample is reduced. Moreover, the sample's elastic deformation can be suppressed by $r = 0$ when measuring the sample surface topography. Then, elasticity is estimated accurately using the previous line surface topography without deformation. The block diagram of the proposed method is shown in Fig. 7.

## IV. SIMULATION AND EXPERIMENT RESULTS

In this section, we verify the effectiveness of the proposed method by simulation and experiments.

### A. Simulation results

In this subsection, the effectiveness of the proposal method is verified by simulation. We use the plant model as (5) in this simulation. Fig. 8 shows the simulation results. Fig. 8(a) shows scanning route of probe (only FWS). Fig. 8(b), (c) show the measured surface topography and controller output respectively. In this simulation, reference $r$ is switched between 0 and 0.1 every line. Therefore, the response according to a reference signal arises in the scan of an even number sequence line in at $4 \sim 8$ s and $12 \sim 16$ s in Fig. 8(c)–(e). Fig. 8(f) is the estimation results of sample's spring constant. In this simulation, the sample's spring constant is denoted by

$$k'_a = 1.245 \times 10^8, \tag{26}$$

according to (5). Thus, an acurate estimate is obtained.

### B. Experiment result

Fig. 9 shows experimental results, using the plastic sample. Reference $r$ is switched between 0 and 0.3 every line in this experiment. The triangular signal in Fig. 9(a) shows scanning route of probe (FWS and BWS). In an actual experiment, the piezo actuator has the hysteresis characteristic. In this paper, we assume that this characteristic is small enough and can be ignored. Fig. 9(b), (c) show controller output ($u_i$) and previous line sample surface topography ($d_{i-1}$) respectively, where $\hat{d}_{i-1} = -u_{i-1}$. Fig. 9(d), (e) show plant input ($u_i + \hat{d}_{i-1}$) and output ($z$). sample's spring constant is estimated from plant input and output, using RLS method. Because We only consider FWS, sample's elasticity estimation is not implemented in BWS. Fig. 9(f) shows sample's elasticity ($\hat{k}'_a$) at $0.8 \sim 1.2$ s and $2.3 \sim 2.7$ s, This result is in agreement with (5). Fig. 9 shows 3D mapping of sample surface topography and elasticity by the proposed method.

### C. Evaluation of the proposed method

In this subsection, we evaluate experimental results of proposed method. Fig. 11 shows the evaluation method. The evaluation method is described as follows:

1) Measure sample surface topography and sample's spring constant by the proposed method.
2) Input step signal ($u$) to the plant, and measure plant output ($z$).
3) Create the time–varying system and simulate output ($z_a$) of this system.
4) Compare $z$ and $z_a$.

Measured elasticity is verified if $z_a$ fits in $z$.

From (3), the time–varying system is expressed as

$$\hat{P}(s) = \frac{\hat{k}'_a}{s^2 + b's + k'}. \tag{27}$$

Fig. 12 shows the evaluation results. Fig. 12(a), (b) show surface topography and sample' spring constant. We input a step signal to this plant , shown as Fig. 12(c). Fig. 12(d) shows the comparison of $z$ and $z_a$. From Fig. 12(d), $z_a$ fits in $z$, therefore it is can be concluded that the elasticity estimation is accurate.

## V. CONCLUTION

In this paper, we propose a new method to estimate sample surface topography and elasticity using previous line surface topography by contact–mode AFM. Switching reference shows the advantage to improve S/N ratio. Moreover, we can suppress the influence of elastic deformation, and measure elasticity accurately. In future works, the elasticity estimation will be taken into account based on more precise model of AFM, considering sample's viscosity.. Furthermore, it is necessary to extend our approach to dynamic–mode AFM, which can reduce the force to soft material.

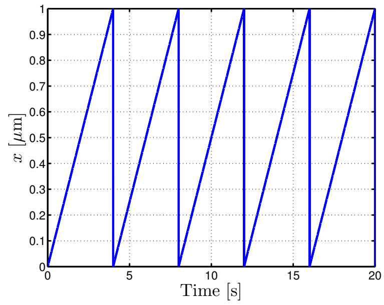


(a) Scanning ($x$).

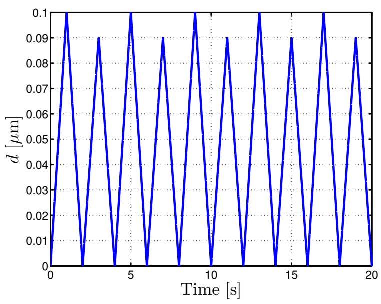


(b) Surface topography ($d_i$).

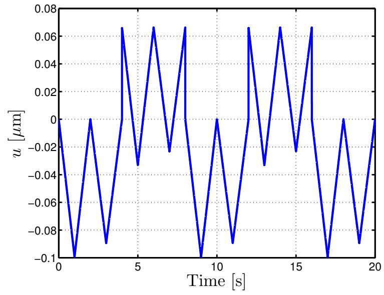


(c) Controller output ($u_i$).

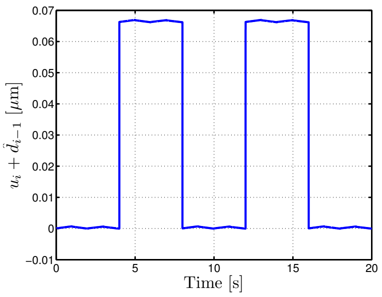


(d) Plant input ($u_i + \hat{d}_{i-1}$).

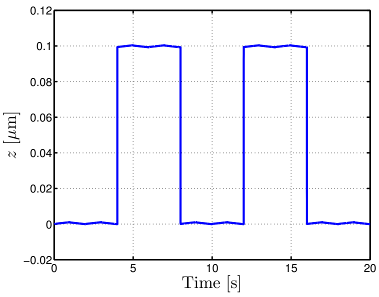


(e) Plant output ($z$).

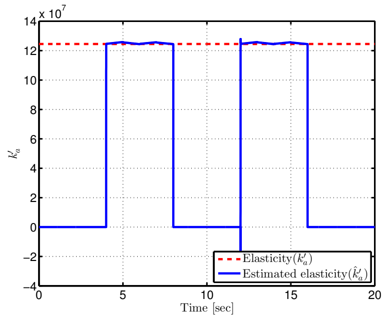


(f) Estimated elasticity ($\hat{k}_a'$).

Fig. 8. Simulation results.

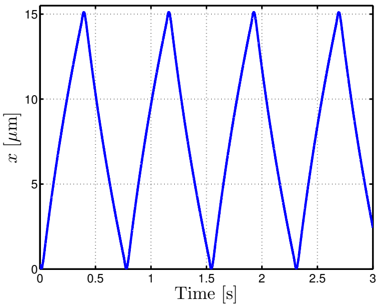


(a) Scanning ($x$).

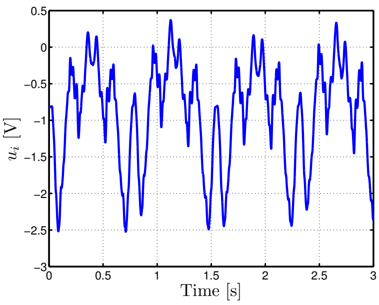


(b) Controller output ($u_i$).

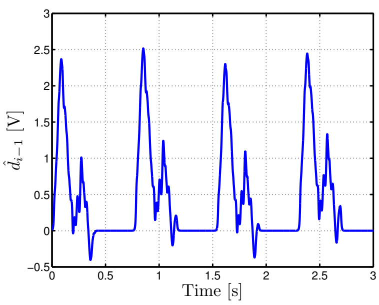


(c) Previous line surface topography ($\hat{d}_{i-1}$).

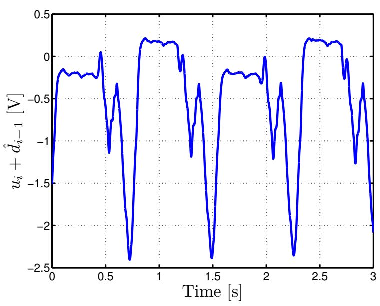


(d) Plant input ($u_i + \hat{d}_{i-1}$).

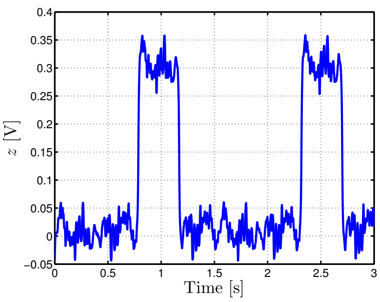


(e) Plant output ($z$).

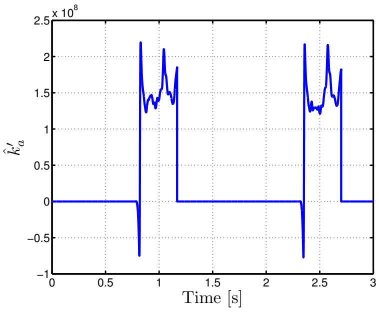


(f) Estimated elasticity ($\hat{k}_a'$).

Fig. 9. Experimental results.

## References


[1] C. Onal, C. Pawasche, M.Sitti, "A scaled bilateral control system for experimental 1-D teleoperated nanomanipulation applications", Intelligent Robots and Systems, pp. 483–488, 2007

[2] T. Ando, "Control Techniques in High-speed Atomic Force Microscopy", American Control Conference, pp. 3194–3200, 2008

[3] A. Fleming, "A Method for Reduction Piezoelectric Non–Linearity in Scanning Probe Microscope Images", American Control Conference, pp. 2861–2866, 2011

[4] G. Schitter, P. Thurner, P. Hansma, "Design and input-shaping control of a novel scanner for high–speed atomic force microscopy", Mechatronics, Vol. 18, pp. 282–288, 2008

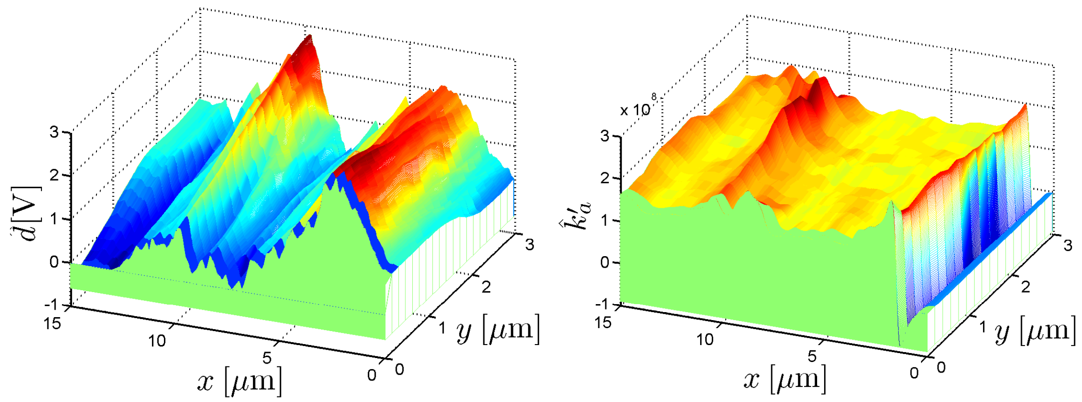


(a) 3D map of surface topography ($\hat{d}$). (b) 3D map of elasticity ($\hat{k}'_a$).

Fig. 10. 3D mapping of the sample.

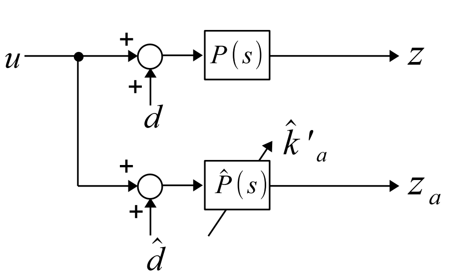


Fig. 11. Block diagram of the evaluation method.

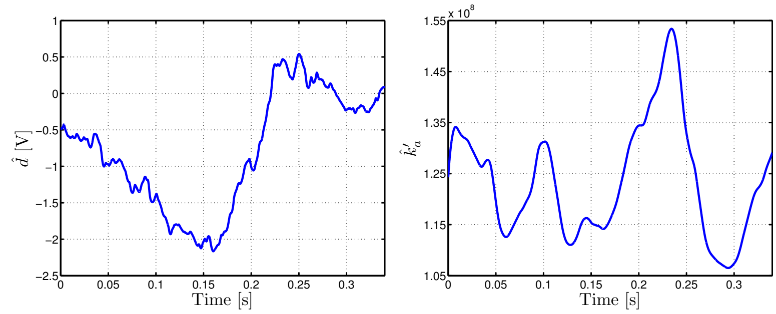


(a) Surface topography ($\hat{d}$). (b) Estimated elasticity ($\hat{k}'_a$).

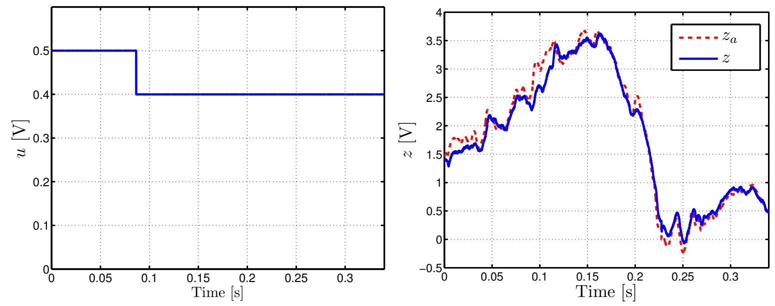


(c) input signal ($u$). (d) Compared result ($z$, $z_a$).

Fig. 12. Experimental results of the evaluation method.


[5] I. Mahmood, S. Moheimani, "Improvement of accuracy and speed of a commercial AFM using positive position feedback control", American Control Conference, pp. 973–978, 2009

[6] T. Shiraishi, H. Fujimoto, "High-Speed Atomic Force Microscope by Surface Topography Observer", Japanese Journal of Applied Physics, Vol. 51, pp. 026602–026602–7, 2012

[7] H. Fujimoto, T. Oshima "Contact–mode AFM Control with Modified Surface Topography Learning Observer and PTC", 34th Annual Conference of the IEEE Industrial Electronics Society, pp. 2515–2520, 2008

[8] K. Nakajima, S. Fujinami, D. Wang, T. Nishi, "Evaluation of Viscoelastic Properties of Polymeric Materials by Atomic Foece Microscopy", Journal of the Japan Society of Colour Material, Vol. 83, pp. 108–114, 2010 (in Japanese)

[9] H. Sekiguchi, A. Hidaka, Y. Shiga, A. Ikai, T. Osada, "High–sensitivity detection of proteins using gel electrophoresis and atomic force microscopy", Ultramicroscopy, Vol. 30, pp. 351–356, 2009 (in Japanese)

[10] D. Kim, J. Park, M. Kim, K. hong, "AFM-based identification of the dynamic properties of globular protein : simulation study", Journal of Mechanical Science and Technology, Vol. 22, pp. 2203–2212, 2008

[11] "Roadmap of Elasticity Measurement by AFM",Japan Society for the Promotion Science nanoprobe technology 167 committee, 2012

[12] A. Sebastian, M. Salapaka, D. Chen, J. Cleveland, "Harmonic analysis based modeling of tapping mode AFM" , American Control Conference, Vol. 1, pp. 232–236, 1999

[13] H. Fujimoto, B. Yao, "Multirate adaptive robust control for discrete-time non-minimum phase systems and application to lineaar motors", IEEE/ASME Transaction on Mechatronics, Vol. 10, pp. 371–377, 2005